

Screening for AVA anomalies in siliciclastic basins: testing a seismic inversion method in the Mississippi Canyon, Gulf of Mexico

David Went^{1*}, Richard Hedley¹ and Jon Rogers¹ demonstrate a highly effective method to identify hydrocarbons without any well data control in the simply buried Neogene and Paleogene (Tertiary) strata of the Mississippi Canyon.

Abstract

The results of a seismic inversion method designed to screen for AVA anomalies in siliciclastic frontier basins is tested in a mature deep-water setting, the Mississippi Canyon, Gulf of Mexico. The method, which is founded on a universal rock property model for siliciclastic sediments, uses widely available partial stacks to invert seismic data for intercept and gradient impedances and generate a relative elastic inversion volume (rEEI), optimised for lithology and fluid detection. The results demonstrate the method is highly effective, but not infallible, at identifying hydrocarbons without any well data control in the simply buried Neogene and Paleogene (Tertiary) strata of the Mississippi Canyon. They further suggest that the use of the method in the early stages of prospecting in simply buried, siliciclastic basins globally, has the potential to identify opportunities that might otherwise be overlooked when interpreting only on the full stack.

Introduction

The search for large oil and gas accumulations increasingly relies on prospecting for stratigraphic rather than structural traps,

commonly in deep water, in passive margins (Allan et al 2006). Delimiting sand fairways and high grading closures with oil and gas potential increasingly relies on amplitude variation with angle (AVA) analysis. In the traditional approach to prospecting, detailed AVA analysis is performed on a few highly ranked prospects identified from integrated G&G studies, commonly in the latter stages of the exploration cycle. A simple but robust method for screening for AVA anomalies in the early stages of exploration, for example in frontier siliciclastic basins which typically lack calibrating wells, is an alternative approach, described and tested in this article. A seismic inversion method is used that seeks to exploit a globally applicable rock property model, designed to discriminate lithology and fluid using AVA (Went 2021). Although the method is ideally suited to frontier siliciclastic basins, the efficacy of the method is difficult to prove or quantify in such a setting. The purpose of this paper is to present the results of an experiment conducted to test the model and method in a more mature area: the deep-water, Mississippi Canyon, Gulf of Mexico, where there are numerous discoveries and readily accessible well data. The results show that the AVA model

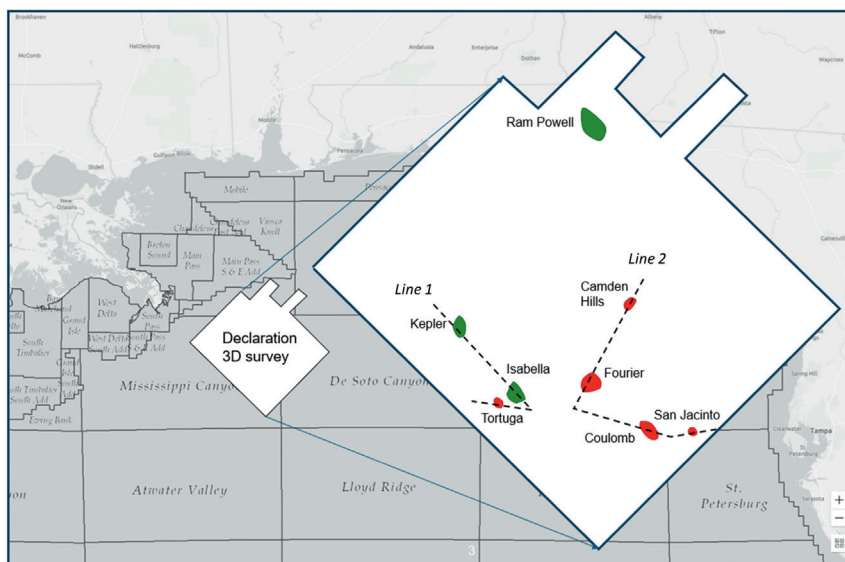


Figure 1 Location of the test dataset (Declaration Refocus) in the offshore deepwater Gulf of Mexico (Mississippi Canyon, De Soto Canyon and Vioska Knoll Protraction Areas). The expanded survey image shows the lines of section and the fields mentioned in the text and figures.

¹ TGS Geophysical Company ASA

* Corresponding author, E-mail: davewent@tgs.com

DOI: xxx

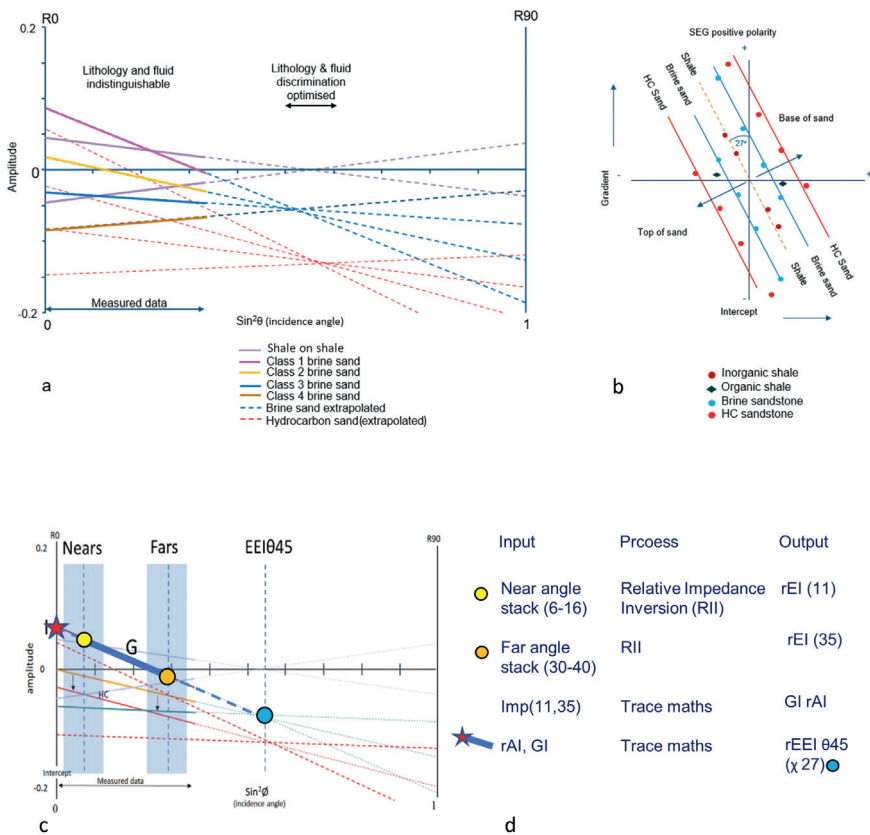


Figure 2 a) Generic or universal rock property half-space model for sands and shales based on global average rock property data (Went 2021). The forward model suggests a projection of intercept-gradient to $45^\circ\theta$ should discriminate shale from brine sands and brine sand from hydrocarbon-bearing sands; b) the same data plotted on an intercept – gradient cross-plot trends at $27^\circ\chi$ (chi); c) data from partial stacks is used to do the inverse (or reverse) process to calculate gradient, intercept and an extrapolated attribute at $\theta=45^\circ$; d) tabulated summary of the process steps: note the rEI attribute can be calculated using a projection (as shown) or a co-ordinate rotation (as advocated by Whitcombe et al 2002); the values are different but the resulting image is the same (ie they differ only in scale). Linear projection is limited to incidence angles -90 to $+90$ ($\sin^2\theta -1$ to 1).

Field	Well	Well Pay Interval		Thickness		Anomaly	Seismic Pay Indicator	
		Top	Base	Gross	Net Pay		Top	Base
		m SS	m SS	m	m	rEEI450(χ 27)	m	m
Tortuga	MC561-2	4244	4250		6	Y	4250	4300
Isabella	MC562-1	5537	5552		15	Y	5480	5530
		5738	5780	42	35	Y	5700	5750
Kepler	MC383-1	3683	3698		15	Y	3650	3700
		3900	3904		4	Y	3850	3900
Camden Hills	MC348-1	4158	4211	53	12	Y	4200	4250
		4371	4384		12	Y	4350	4400
Fourier	MC522-1	3957	3993	37	9	Weak	3950	4000
		4237	4268	30	12	Y	4225	4275
		4457	4618	162	41	Y	4450	4600
		4938	4975	37	22	Y	4900	4950
Coulomb	MC657-1	5193	5213		20	Y	5000	5050
San Jacinto	DC618-1	4106	4113		7	Y	4100	4150
		4530	4551		21	Y	4475	4525
		4576	4619	43	14	Y	4575	4625
Ram Powell	VK956-1	3826	3846		20	Y	3850	3900

Table 1 Hydrocarbon pay zone analysis for the discovery wells discussed in the text and displayed in the illustrations. The pay zones are compared with the seismic anomalies on the attribute rEEI450 ($27^\circ\chi$), which is hypothesised to be the optimal seismic hydrocarbon indicator. Stacked pays are common. Pay zones in wells less than 3 m thick are not included.

and seismic method, based on widely available partial stacks, is highly effective at identifying hydrocarbons in the Paleogene and Neogene (Tertiary) strata of this simply buried siliciclastic basin. The adoption of the method in the early stages of prospecting, in suitable frontier basins globally, has the potential to identify opportunities that are otherwise hard to identify when interpreting only on the full stack.

Geological setting

The Gulf of Mexico is filled with more than 20 km of sediment. Approximately 2 km of salt filled the centre of the basin immediately prior to the main rift event in the Middle Jurassic period. In the Late Jurassic and Cretaceous periods, the northern margin of the basin was characterised by carbonates, deposited in a variety of shelf, slope and basinal settings. By the early Tertiary period, the Laramide Orogeny caused uplift of the Rocky Mountains and consequently, large river systems were established that drained the North American continent, dispersing southwards. Large amounts of siliciclastic sediment were, thereby, emptied into the Gulf of Mexico. These Tertiary-aged sediments were deposited by several large delta – submarine fan systems, similar to the present-day Mississippi. Beyond the deltas, sediments passed through a series of mini basins created by the movement of the underlying salt. Salt movement generated numerous rim synclines and turtlebacks and resulted in the formation of numerous types of structural and stratigraphic trap (Bouroulllec et al. 2017).

The area covered by this study contains up to 10 km of Cretaceous and Tertiary sediments. Although a significant number of large oil fields have been found in Middle Jurassic clastic sediments that rest on the autochthonous salt, the Norphlet play (Godo 2019), most of the oil and gas discoveries have been made in the Tertiary-aged siliciclastic sediments. It is the Tertiary-aged strata that form the subject of this investigation.

The area covered by the inverted 3D seismic data is shown in Figure 1. It is in the Mississippi Canyon, the western part of the DeSoto Canyon and southernmost part of the Vioska Knoll Protraction Areas. The survey is called Declaration Refocus and is a composite 3D volume reprocessed in 2019 and 2020. It amalgamated two orthogonal 3D WAZ acquisitions acquired by TGS using the WesternGeco Q-Marine and CGG StagSeis seismic systems. The survey covers 8885 km² and was processed through a sequence using the latest in 3D deghosting and demultiple techniques together with dual passes of Dynamic Matching Full-Waveform Inversion (DM-FWI) (Tiwari et al 2018).

Method

The approach combines application of a universally applicable rock property model with a practical method for reliably performing AVA inversion using partial stacks of 3D seismic data. Prior to inversion, the pre-stack seismic data underwent a light conditioning workflow performed in the time domain, including Q-compensation, mapping to angle domain, timing alignment, median filtering and wavelet

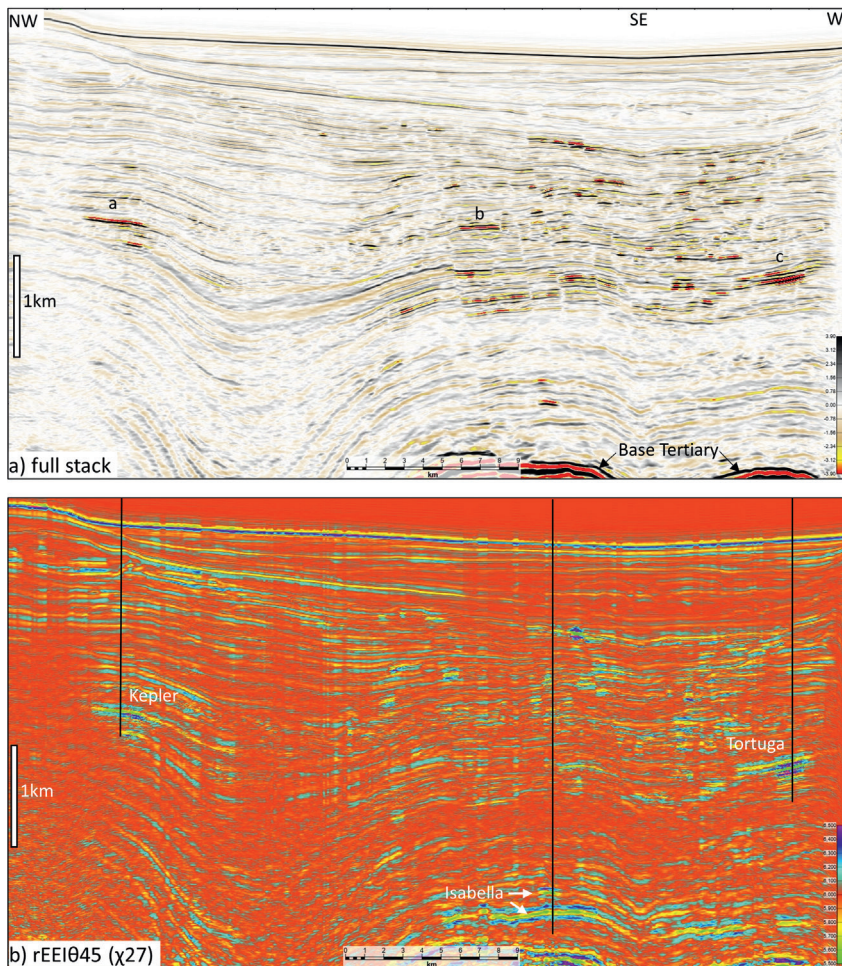


Figure 3 Arbitrary line 1 through the 3D survey: a) full depth-migrated stack, b) elastic inversion, $rEEI45^{\circ}0$ (χ^27). Numerous amplitude anomalies are present in the full stack. Three are highlighted with letters, a, b and c. Amplitude anomalies a and c stand out strongly on the $rEEI45^{\circ}0$ volume and are confirmed as Class III AVA anomalies on AI-GI cross-plots (Figure 4d and f). They correspond with Kepler (oil) and Tortuga (gas) fields. Not all amplitude anomalies (bright spots) are AVA anomalies, as exemplified by full stack amplitude anomaly b which is not anomalous on $rEEI45^{\circ}0$ (or an AI-GI cross-plot). An extensive AVA anomaly is indicated deep in the Tertiary section in $rEEI45^{\circ}0$. This is not associated with a full stack amplitude anomaly but is anomalous on an AI-GI cross-plot where it plots as a Class II AVA anomaly. It corresponds with the main oil pay in Isabella. The small AVA anomaly above it is a gas-bearing sand showing Class III AVA (Figure 5). See Figure 4a for confirmation of our categorisation of AVA classes in cross-plot space.

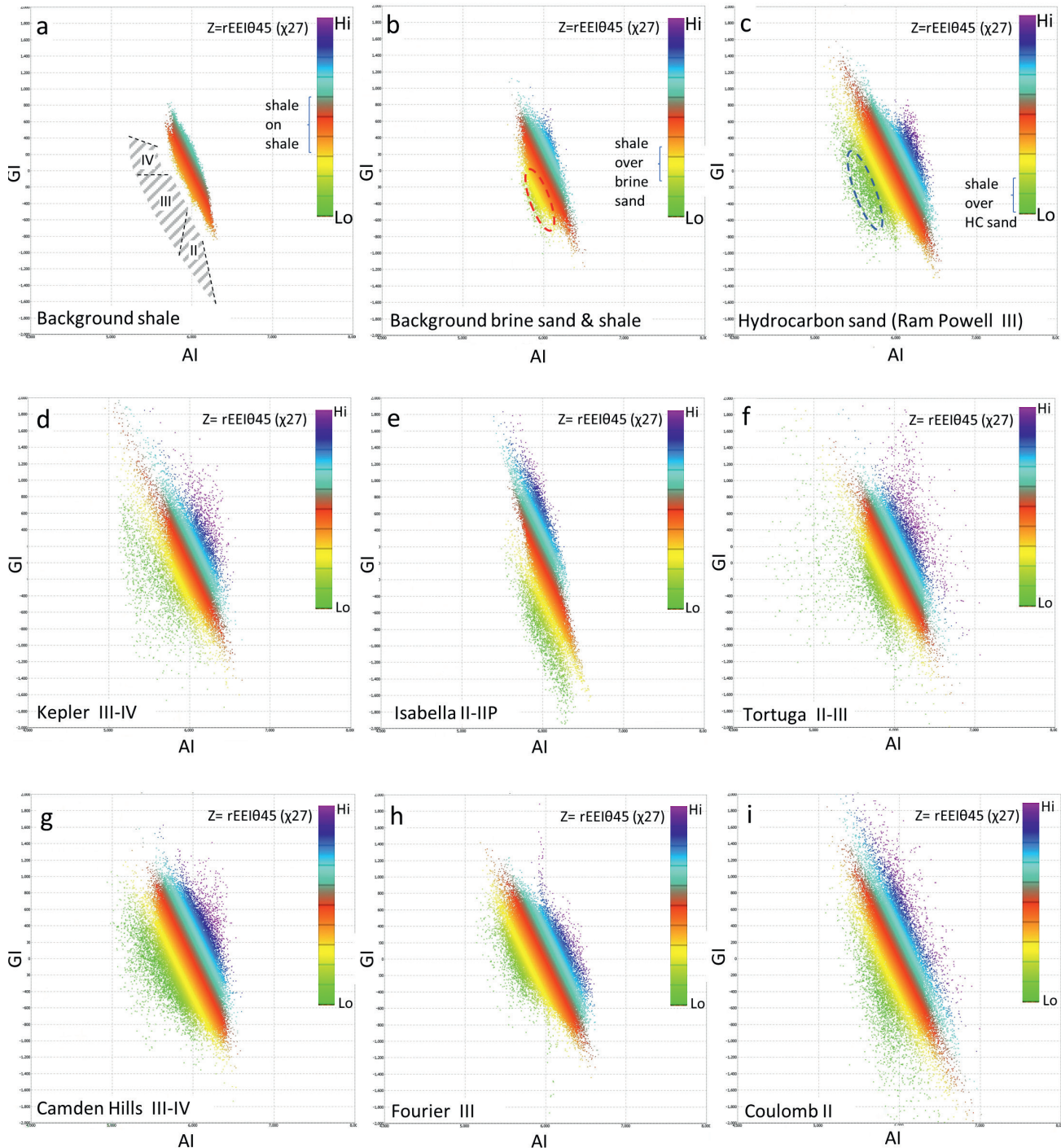


Figure 4 Cross-plots of AI vs GI coloured coded by rEEI χ_{27} ($=\theta_{45}$), from selected localities (cubes of data) in the 3D survey: a) typical shale background response (red is dominant on rEEI45° seismic sections). The shaded areas show the position of anomalous AVA data of our Classes II, III and IV respectively, b) shale and brine sand response (yellow-red-blue on rEEI45° seismic sections), c) hydrocarbon sand response (green on rEEI sections) of Class III type, Ram Powell Field, d) Class III-IV AVA anomaly, Kepler Field, e) Class II/IIP AVA anomaly, Isabella Field, f) Class II-III AVA anomaly, Tortuga Field, g) Class III-IV AVA anomaly, Camden Hills Field, h) Class III-IV AVA anomaly, Fourier Field, i) Class II AVA anomaly, Coulomb Field. Note all cross-plots are scaled similarly with x (AI) and y (GI) to true scale (one unit of x = one unit of y), and the χ -angle colour-coding a true 27°.

domain bandwidth extension. These angle domain data ranging from 0 - 50° in 2° increments were then used to construct near and far sub-stacks, 6-16° and 30-40°, respectively.

The justifications and development of a universal rock-property forward model for siliciclastic strata was presented in some detail by Went (2021). These arguments are not repeated here. However, the generic forward-model, summarised in angle-de-

pendent reflectivity and intercept versus gradient cross-plot formats, is shown in Figure 2a and b. The implication of the generic model is that a reliable two-term inversion for intercept and gradient, projected to 45° incidence angle (equivalent to a 27° angle on an intercept gradient cross-plot), should capture most anomalies of interest between 1000 and 3500 m below seabed in simply buried siliciclastic basins.

The inversion method, concept and workflow are summarised in Figure 2c and d. A statistical wavelet is extracted from each partial stack over the interval of interest. A band-limited inversion is then performed to remove the wavelet (and conduct any phase correction) using a model-based inversion with a uniform background impedance of 6 GPa. This results in near and far angle stack impedance volumes which represent band-limited, elastic impedance at (in this case) 11° and 35° respectively (cf. Connelly 1999). Calculation of the rate at which impedance changes with angle yields an estimate of the gradient (the gradient impedance volume, GI) and the near stack impedance and gradient impedance volumes are combined (re-weighted) to generate the intercept impedance volume (relative acoustic impedance, AI). The AI and GI volumes are combined to produce relative extended elastic impedance (rEEI) for any projected angle of incidence (θ) or cross-plot rotation angle (χ). The most pertinent angle for lithology and fluid detection is $45^\circ\theta$ or $27^\circ\chi$ (cf. Whitcombe et al 2002). Since the $rEEI45^\circ\theta$ ($27^\circ\chi$) volume is a representation of the position of the data on an AI-GI cross plot, it can be used to screen for anomalies directly, without recourse to AVA cross-plotting or anxiety over interpretation of phase and polarity, as is commonly the case when interpreting on reflection data.

Results

The seismic data were screened for amplitude and AVA anomalies using the full stack and $rEEI45^\circ\theta$ ($27^\circ\chi$) volumes. The location of prominent anomalies was compared with the location of known oil and gas fields shown on scout maps. Many of the fields showed good rEEI anomalies, prompting a more detailed analysis, including identification of the pay zones in the wells and comparison of the depths of pay in the wells with the depth of the anomalies seen in the seismic inversion (Table 1). Two representative lines of section through anomalies and fields are presented to illustrate the results (Figure 1).

The first line passes through the fields Kepler, Isabella and Tortuga (Figure 3). The illustrated interval shows numerous full stack amplitude anomalies (bright spots). Three of the more

extensive ones are highlighted with the letters a, b and c. Comparison of the full stack and inverted volume $rEEI45^\circ\theta$ ($27^\circ\chi$), reveals that full-stack amplitude anomalies a and c correspond with $rEEI45^\circ\theta$ ($27^\circ\chi$) anomalies over the proven fields Kepler (which has two pay zones) and Tortuga. Amplitude anomaly b, however, is undrilled and does not show an anomalous rEEI response. It highlights that not all stack amplitude anomalies are AVA anomalies. AI-GI cross plots from the Kepler and Tortuga anomalies confirm the anomalous AVA character and further indicate that Kepler and Tortuga show Class III-IV and Class II-III type AVA anomalies respectively (Figure 4d and f) (Castagna and Swan 1997).

Deep in the Tertiary section on line 1 there is little in the way of anomalous full-stack amplitude behaviour. However, on the inverted $rEEI45^\circ\theta$ ($27^\circ\chi$) volume there is an extensive prominent anomaly. Comparison with known discoveries reveals this anomaly corresponds to 35 m of oil pay in the Isabella discovery (Figure 5). A cross-plot of AI versus GI confirms the presence of an AVA anomaly and further suggests the oil sand to be a Class II/IIP anomaly, consistent with the weak full stack response (Figure 4e) (Rutherford and Williams 1989). A small bright spot 200 m above the oil pay anomaly represents a gas sand which also shows anomalous AVA behaviour, of Class III type. The Isabella discovery is a good example of what is possible when screening for AVA anomalies that do not illuminate brightly on the full stack.

The second line passes through the fields Camden Hills, Fourier, Coulomb and San Jacinto (Figure 6). The main bright events on the full stack relate to the highly reflective carbonates at the top of the Mesozoic sequence and the cap of the salt diapirs (Figure 6a). Aside from these non-siliciclastic lithologies, bright spots are also present in the Tertiary section. Significant anomalies are labelled a, b, c and d. The full stack anomalies a, b, and d are also $rEEI45^\circ\theta$ ($27^\circ\chi$) anomalies (Figure 7b). Camden Hills, Fourier and San Jacinto all show multiple stacked pays, the intervals of which correspond closely to the indications of pay in the seismic inversion (Table 1). Cross plots of AI versus GI confirm

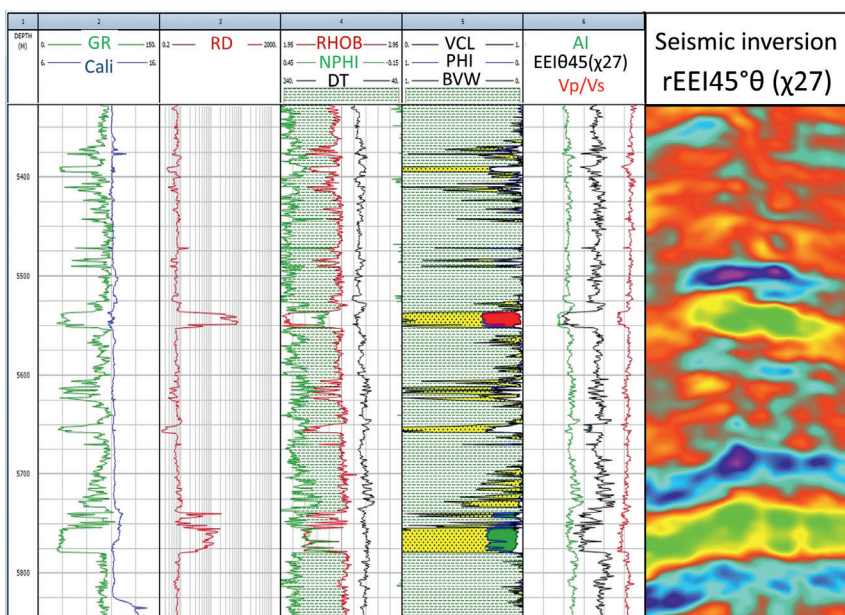


Figure 5 Petrophysical analysis of the deep Tertiary section in Isabella well MC562-1 showing lithology, porosity, resistivity, and seismic logs (AI, $EEI_{\chi 27}$, V_p/V_s). The well data pay zones and $rEEI45^\circ\theta$ (χ_{27}) logs closely match the results of the band-limited seismic inversion, $rEEI45^\circ\theta$ (χ_{27}).

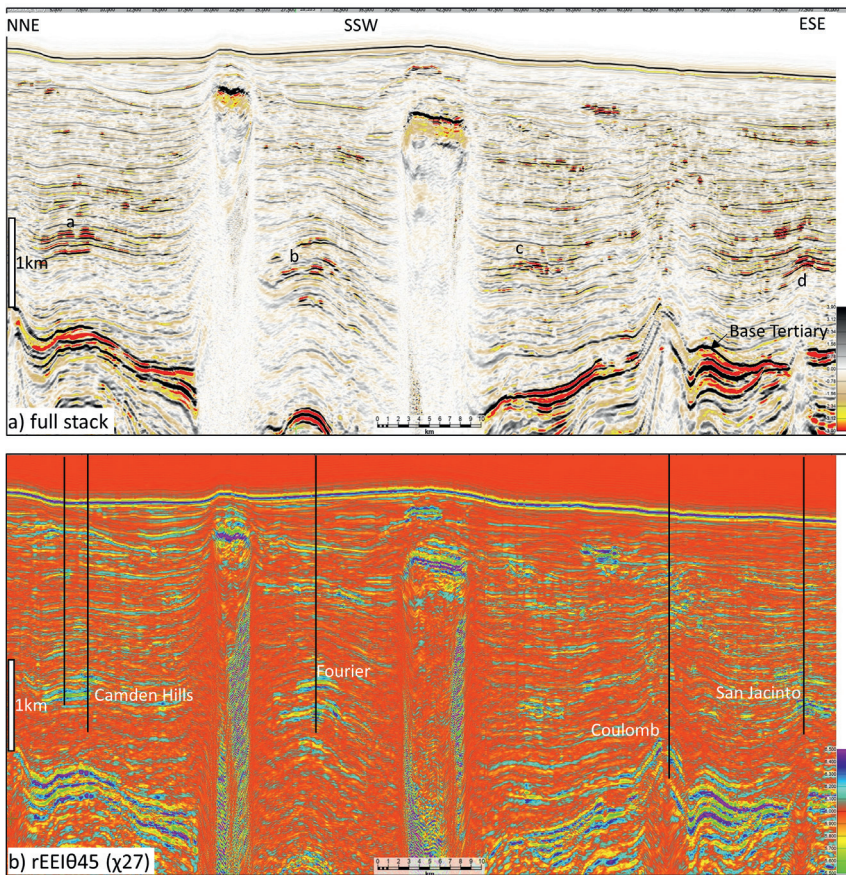


Figure 6 Arbitrary line 2 through the 3D survey: a) full depth-migrated stack, b) elastic inversion, rEEI45°θ (χ=27). Numerous amplitude anomalies are present in the full stack. Four are highlighted with letters, a, b, c and d. Amplitude anomalies a, b and d stand out strongly on the rEEI45°θ volume and are confirmed as Class III AVA anomalies on AI-GI cross-plots (Figure 4). They correspond with Camden Hills, Fourier, and San Jacinto fields. Full stack amplitude anomaly c, which looks comparable to b in the full stack, is not a strong AVA anomaly on rEEI45°θ. A pronounced AVA anomaly is indicated deep in the Tertiary section in rEEI45°θ at Coulomb Field. This is not associated with a full stack amplitude anomaly but is anomalous on an AI-GI cross-plot, where it is confirmed as a Class II AVA anomaly. It further confirms not all AVA anomalies are anomalous on the full stack.

19 Fields have good rEEI anomalies

- Kepler
- Isabela
- East Anstey
- N Hershel
- Santiago
- Dalmatian
- Dalmatian South
- Ram Powell
- King
- Fourier
- Fastball
- Tortuga
- Pompano
- Coulomb
- Camden Hills
- San Jacinto
- Blind Faith
- Ariel
- Troubadour

3 wells drilled on rEEI anomalies but were dry

- 606-1
- 476-1
- 786-1

6 Discoveries with no rEEI anomaly

- Nidermeyer
- Macondo
- Odd Job
- Gemini (salt flank)
- Hoffe park (salt flank)
- Herschel (salt flank)

Data suitability issues

$$\frac{19}{22} = 85\% \text{ of rEEI anomalies drilled are oil/gas fields}$$

Figure 7 Evaluation of drilled rEEI45°θ anomalies in the Tertiary section of the study area seismic data. The success rate is good, but not perfect. Furthermore, there are six fields which do not show as anomalies, due to illumination issues associated with data acquisition.

these are Class III or III-IV type anomalies (Figure 4g and h). The bright spot c is associated with a weak rEEI45°θ (27°χ) response typical of a lithology effect (shale over sand, Figure 4b). It is a further reminder, not all bright spots are AVA anomalies. Deeper in the section an rEEI45°θ (27°χ) anomaly is present over the Coulomb Field. This AVA anomaly is not associated with a bright spot but is co-incident with pay present in the discovery well (Table 1). The AI-GI cross plot over Coulomb confirms a Class II type AVA anomaly, thereby explaining the absence of a strong bright response on the full stack. As with Isabella, it is a good example of the power of AVA to identify opportunities that might otherwise be overlooked if working solely with the full stack.

Analysis – success rates and risks

A comparison of the seismic inversion with other fields in the survey area was conducted using the same approach described above. We have determined that approximately 85% of identified prominent anomalies in the Tertiary section in the data volume, that have been drilled, have been oil or gas discoveries (Figure 7). However, three rEEI45°θ (27°χ) anomalies, representing the remaining 15%, have been tested by the drill bit and declared dry. Investigating further, two of the three wells, MC606-1 and MC476-1, were not truly dry. They contained hydrocarbons at the level of the rEEI anomalies but in insufficient quantities or saturation to be declared commercial.

The third well, MC786-1 encountered good sands but no indications of hydrocarbons at all. These results indicate that AVA analysis is not without ambiguity or difficulty. Interpretations and judgments have to be made on data quality, the causes of anomalies (e.g. are they the result of lithology or fluid effects), and the additional risks associated with drilling them (such as pay thickness and oil saturation). The results of this analysis serve to indicate that the AVA method, whilst good at determining the presence of hydrocarbons, is not infallible. Furthermore, the method is not applicable in all circumstances. There are six fields in the Tertiary age strata which do not illuminate as anomalies on either the full stack or the rEEI45°0 (27° χ) volume. In these cases, the problem stems from data acquisition and a lack of signal. In some cases, this is demonstrably due to the fields being in the shadow of salt bodies (stocks and canopies). It is the geology and its impact on data quality that is the limiting factor in this case, not the method. Finally, there are 11 discoveries in the deep Mesozoic Norphlet play (Godo 2019). Here, gross lithology and depth are limiting factors; the clastic reservoirs occur interbedded with carbonates and are at depths typically exceeding 6000 m.

Conclusions

Proof testing of a seismic inversion method designed to screen for AVA anomalies in siliciclastic frontier basins has been successfully conducted on a 3D dataset in a mature deep-water setting, the Mississippi Canyon, Gulf of Mexico. The method, which is founded on a universal rock property model for siliciclastic sediments, uses widely available partial stacks to invert seismic data for intercept and gradient impedances and to generate a relative extended elastic impedance volume (rEEI) optimised for lithology and fluid detection. The model suggests an inversion for rEEI45°0 (χ 27°) should identify hydrocarbons in a simply buried Tertiary basin. Such an inversion in the study area was successful in identifying commercial hydrocarbons in approximately 85% of drilled occasions where data was suitable for the process to work.

The results suggest the method could be applied successfully in the early stages of prospecting in comparable, simply buried, siliciclastic basins globally. The method has the potential to identify opportunities that might otherwise be overlooked when interpreting only on the full stack.

Acknowledgments

We wish to thank TGS for permission to publish and Marianne Rauch for her critical review of the results illustrated in this paper.

References

- Allan, J.R., Sun, S.Q. and Trice, R. [2006]. The deliberate search for stratigraphic and subtle combination traps: where are we now? *Geological Society, London, Special Publications*, **254**, 57-103.
- Bouroullec, R., Weimer, P. and Serrano, O. [2017]. Petroleum geology of the Mississippi Canyon, Atwater Valley, western DeSoto Canyon, and western Lloyd Ridge protraction areas, northern deep-water Gulf of Mexico: Traps, reservoirs, and tectono-stratigraphic evolution. *AAPG Bulletin*, **101**, 1073-1108
- Castagna, J.P. and Swan, H.W. [1997]. Principles of AVA cross-plotting: *The Leading Edge*, **16**, 337-344.
- Connolly, P., 1999. Elastic impedance. *The Leading Edge*, **18**, 438-452.
- Godo, T. [2019]. The Smackover–Norphlet petroleum system, deepwater Gulf of Mexico: oil fields, oil shows, and dry holes. *Gulf Coast Association of Geological Societies*, 104-152.
- Rutherford, S.R. and Williams, R.H. [1989]. Amplitude-versus-offset variations in gas sands. *Geophysics*, **54**(6), 680-688.
- Tiwari, D., Mao, J. and Ma, X. [2018]. Refraction and reflection FWI for high-resolution velocity modelling in Mississippi Canyon. 88th Annual International Meeting, *SEG, Expanded Abstracts*, 1288-1292.
- Went, D. [2021]. Practical application of global siliciclastic rock-property trends to AVA interpretation in frontier basins. *The Leading Edge*, **40**, 454-459.
- Whitcombe, D.N., Connolly, P.A., Reagan, R.L. and Redshaw, T.C. [2002]. Extended elastic impedance for fluid and lithology prediction. *Geophysics*, **67**(1), 63-67.

ADVERTISEMENT

to be filled by EAGE - 171x77 mm

NAME COMPANY

to be filled by EAGE